ISRM International Symposium
Eurock 2025 – Expanding the Underground Space
Trondheim, Norway, 16-20 June
ISBN 978-82-8208-079-8

Back analysis of a rockfall catalog using radar tracking

A.Y. Xie & B.Q. Li
Western University, London, Ontario, Canada
arnold.xie@uwo.ca

Z. Huang
Rocscience Inc., Toronto, Ontario, Canada

Abstract

Reliable estimates of rockfall hazards have a significant impact on the design of roadways, slopes, open pits, and underground excavations. The reliability of these estimates is dependent on numerical models calibrated on rockfall catalogs. Recent advancements in radar technology enable high-resolution monitoring of rockfall events and provide valuable data on their propagation. However, few methods are available to efficiently process these radar data and leverage them for back analysis. Hence, we use a grid search for back analysis of coefficients of restitution (CORs). The framework is demonstrated through a case study of an open-pit mine where a Doppler radar unit was installed and collected a rockfall catalog comprising 21 events and 19356 measured rock positions. Trajectories simulated using the mean and covariance of the best-fit CORs exhibit reasonable agreement with the measured data. This framework enables a rapid assessment of data quality and improves the efficiency and objectivity of back analysis when considering a large catalog of rockfall events.

Keywords

rockfall; remote sensing; numerical simulation; back analysis; calibration;

1 Introduction

Climate change has led to rising temperatures and unprecedent weather extremes that can exacerbate rockfall hazards. For example, Stoffel et al. (2024) found that increasing air temperatures exacerbated the degradation of permafrost over decades, leading to increased rockfall activity. Similarly, Mirhadi and Macciotta (2023) found that climatic changes in precipitation and freeze-thaw cycles has led to more frequent and destructive rockfall events. Viani et al. (2020) studied a century-long catalog of rockfalls in the Western Italian Alps and posited that anomalously high temperatures and rainfall during summer elevated seasonal thawing, resulting in more frequent rockfall events. These studies underscore a dire need for continuous monitoring and mitigation of rockfall hazards given the adverse effects of climate change.

A key component to rockfall hazard mitigation is reliable trajectory estimation, typically achieved through numerical simulations. These simulations incorporate various factors such as rock shape (Caviezel et al. 2021; Zheng et al. 2021), slope geometry (Jaboyedoff et al. 2021; Silveira et al. 2024), and surface roughness (Zheng et al. 2021; Noël et al. 2023), and can be employed to probabilistically assess the wide range of potential rockfall trajectories and impact zones. This level of detail is difficult to achieve through empirical methods such as the Rockfall Hazard Rating System (Pierson et al. 1990).

It is crucial to calibrate these numerical simulations to ensure their reliability (Wyllie 2014a). This process is also termed back analysis, where the constitutive parameters such as normal and tangential coefficients of restitution (Wyllie 2014b; Sabatakakis et al. 2015; Zhao et al. 2024) (CORs), are adjusted until the simulation outputs match the measured data.. These parameters should ideally be site-specific and calibrated by analyzing the historical catalog of rockfall events at a given site (Sabatakakis et al. 2015; Ferrari et al. 2016; Scavia et al. 2020). Manual calibration is often a tedious and time-consuming process (Williams et al. 2020) involving incremental trial-and-error (Budetta et al. 2016; Mineo 2020). This approach is not only labor-intensive but also subjective, as it depends on the expertise and judgment of the individual performing the calibration (Soler et al. 2013; Wyllie 2014a; Mineo 2020).

These limitations have become more pressing in recent years with the advent of automated sensing technologies that generate large volumes of high-quality data. Techniques such as terrain laser scanning (LiDAR) (Pieraccini et al. 2006; Fanos and Pradhan 2016, 2018), photogrammetry (Caviezel et al. 2021; Zhu et al. 2024), thermal camera monitoring (Teza et al. 2015; Blahůt and Racek 2023; Potter et al. 2024), and radar tracking (Carlà et al. 2019, 2024) offer unprecedented detail and accuracy in capturing the non-linear dynamics of rockfall events. High-resolution data from LiDAR and photogrammetry allows for precise mapping of terrain and identification of potential rockfall sources (Pieraccini et al. 2006). Meanwhile, high-frequency monitoring with thermal cameras and radar tracking enables continuous observation of rock faces to detect temperature changes (Teza et al. 2015) or subtle movements (Carlà et al. 2019) that could indicate imminent rockfalls. Specifically, radar is suitable for long-term failure forecasting (Carlà et al. 2019) and real-time warning (Carlà et al. 2024) of rockfall hazards. These applications highlight radar's advantages in high time resolution, wide coverage, and low energy consumption for continuous monitoring. These data would facilitate more precise calibration of the numerical simulations but are difficult to integrate into a back analysis workflow given the volume and variety of information.

Here, we develop a grid-search method based on a quantitative goodness-of-fit metric that measures the similarity between a radar-tracked and simulated rockfall trajectory (Xie et al. 2024). We further demonstrate its efficacy on a large catalog of radar-tracked rockfalls containing 21 independently monitored events from the same 200m x 200 m source region in an open-pit mine. These events consist of a total of 19,356 measured rock positions.

2 Data

Mount Rawdon is an open-pit gold mine located 75 km south-west of Bundaberg, Queensland. 21 independent rockfall events were recorded using a ground-based Doppler radar deployed from May to July 2023. Their mean trajectories and lithology are shown in Figure 1. The cutoff positions of these events exhibit a much larger variation than the initial positions, even though all the rockfall events occurred within the Curtis Island group metasediments (Jele and Sullivan 2016). This consistent lithology motivates the present work to develop a unifying set of CORs that can describe the rich catalogue of rockfall events.

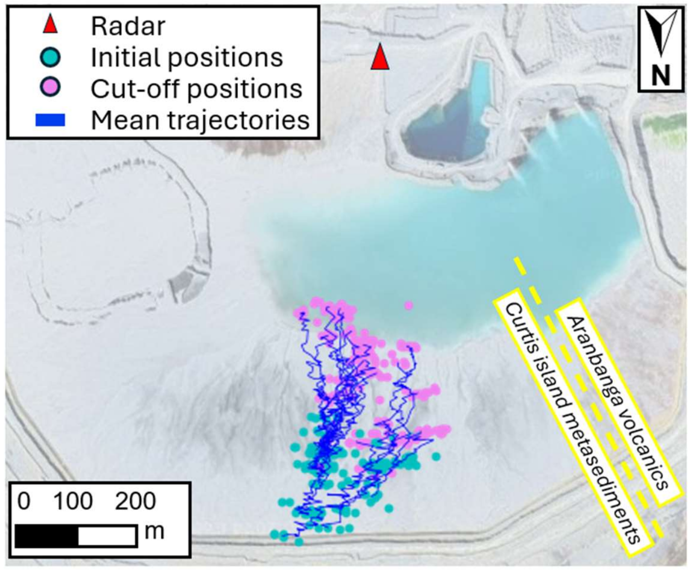

Figure 1 Rockfall catalogue acquired from radar monitoring at the Mount Rawdon gold mine. Lithology information adapted from Jele and Sullivan (2016)

The radar system is *RockSpot* from *IDS GeoRadar* (Viviani et al. 2020). Key technical specifications are listed in Table 1.

Table 1 Technical specifications of the *RockSpot* from *IDS GeoRadar* used for Doppler radar monitoring (Viviani et al. 2020)

Specifications	Values
Operating range	130 m to 2000 m
Tracking range resolution	4 m
Minimal detectable rock speed	1 m/s
Field of view	80° Azimuth, 40° Elevation
Tracking azimuth accuracy	1°
Maximum track update frequency	4 Hz

Key kinematic features of these events are listed in Table 2. Most events occurred at night, necessitating the acquisition of radar data. The events can be divided into two groups according to the trend of their mean trajectories: the first group predominantly falls towards the south with trends ranging from 167.42° to 216.93°, while the second group consists of 3 events trending towards the southwest (indicated in bold font in Table 2).

Table 2 Details of the 21 events in the Mt Rawdon rockfall catalogue. Trend is the azimuth of the initial velocity, where bolded entries indicate the events falling towards the southwest.

Event #	Duration (s)	Number of time steps	Average rocks per scan	Initial speed (m/s)	Trend (°)
1	7.90	18	6.06	8.59	214.93
2	26.51	87	31.07	4.85	208.76
3	22.00	30	7.30	2.88	175.84
4	27.92	44	16.52	6.37	188.31
5	27.35	67	14.93	4.42	167.42
6	27.35	60	10.80	3.52	176.81
7	25.66	77	21.06	3.20	202.07
8	**25.38**	**63**	**8.86**	**4.97**	**225.86**
9	24.82	77	22.48	4.49	180.39
10	17.20	52	18.02	4.31	209.98

11	18.61	49	11.45	3.95	206.69
12	**12.69**	**35**	**14.34**	**5.31**	**235.96**
13	10.72	18	8.39	7.21	211.47
14	**11.00**	**35**	**24.89**	**8.08**	**234.36**
15	12.69	36	31.75	6.67	186.49
16	18.33	55	21.73	4.85	191.45
17	11.00	35	26.51	5.88	207.88
18	11.00	29	12.72	5.44	194.76
19	23.69	78	30.73	4.24	198.62
20	23.12	54	13.31	4.94	190.92
21	5.08	19	14.00	12.32	216.93

Table 2, Figure 1, and Figure 2 illustrate the measured rockfall data in detail. The events exhibit a wide range of durations, cut-off distances, and trends, which may be a result of the variability in terrain roughness and the large origin area of the rockfalls. The data also reveal some technical limitations inherent in this type of monitoring program. Firstly, the rock positions shown in Figure 2 exhibit a level of "banding" as a result of the 4 m spatial resolution, which may bias the calculated mean and standard deviations of the recorded rock positions. Secondly, the time steps are not uniform in length due to the dynamic sampling frequency and field of view, which limits the information available from some events. Finally, the number of rocks measured during an event could vary between time steps as a result of shadowing, secondary rockfalls, or rock fragmentation. These inherent sources of uncertainty limit the accuracy and precision of back analysis and are somewhat mitigated by outlier removal and the probabilistic formulation of the framework. Nevertheless, Figure 2 shows that the outlier removal is generally effective and preserves the main body of the rockfall events. This is important given that the chi-square misfit is sensitive to the calculated standard deviations.

2.1 Data preprocessing

2.1.1 Radar acquisition

Radar (Radio Detection And Ranging) technology detects distant objects by generating electromagnetic pulses at a constant frequency and analyzing the reflected pulses (1943). A full cycle where a series of pulses is generated and received is termed as a scan. The generated pulses propagate as a spherical wave in space. Hence, radar natively only measures the range (distance) and azimuth of the falling rock. The elevation of the object is interpolated by projecting it onto the slope as shown in Figure 3a.Thus, the raw radar data attributes are range, azimuth, and time.

Figure 3b shows a plan view of the radar-tracked data. Each square represents the mean (i.e., average) of rock position measured during each scan. Note that each scan can include multiple falling rocks. We term each scan as a *time step* hereinafter. Multiple scans result in a mean trajectory with a standard deviation at each time step. This probabilistic formulation allows us to then quantify the uncertainty of the back-analyzed CORs.

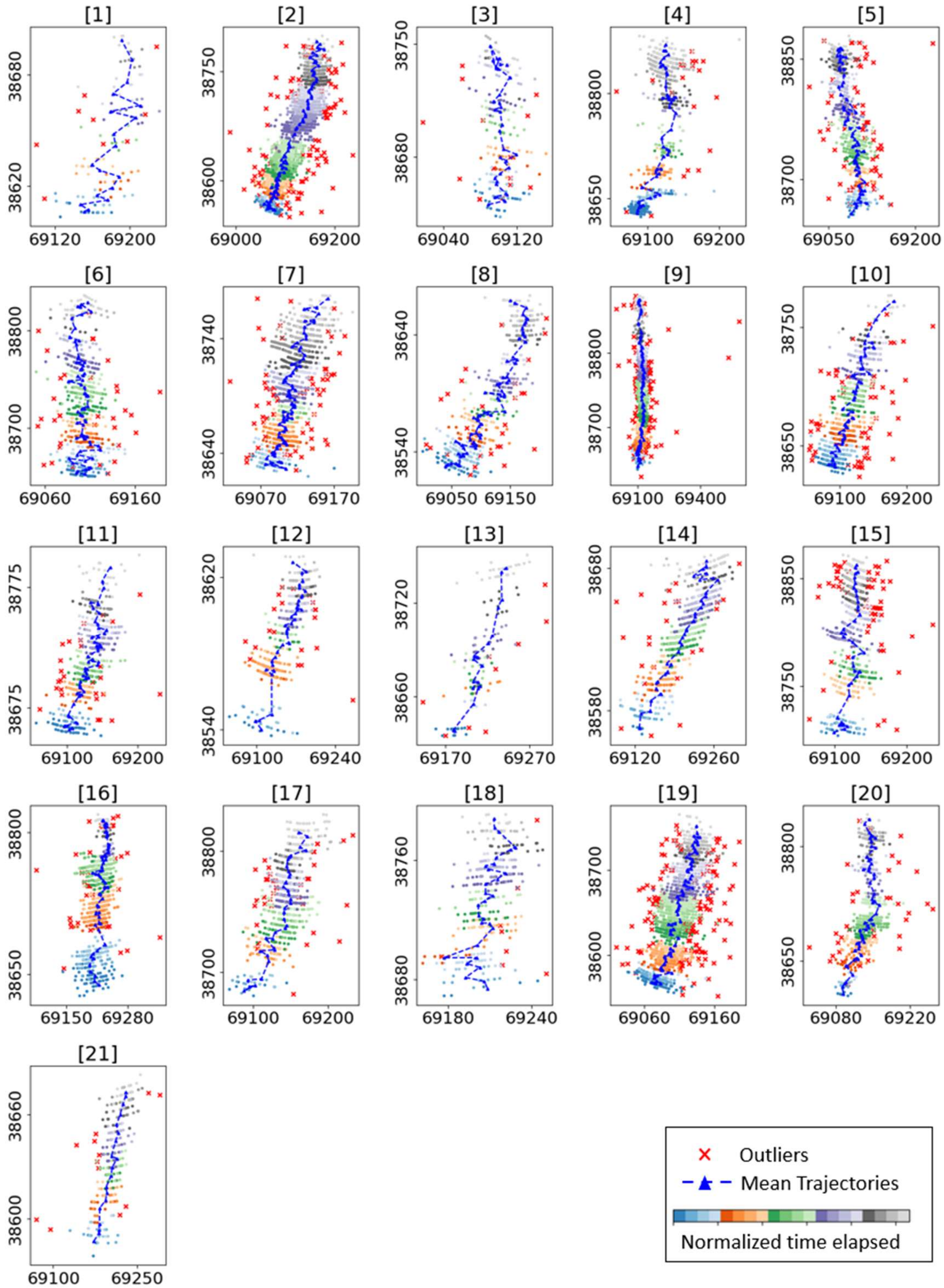

Figure 2 Measured falling rock positions during each rockfall event.

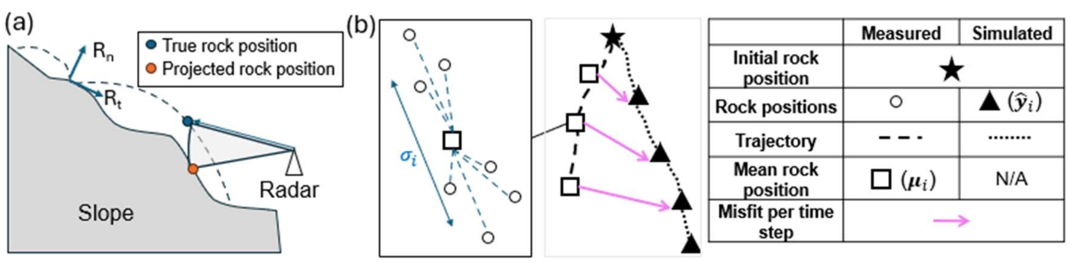

Figure 3 Schematic illustration of (a) radar data acquisition and (b) calculation of misfits between measured and simulated trajectories (Xie et al. 2024).

2.1.2 Outlier removal

Radar monitoring is inherently noisy and may track other moving objects irrelevant to the main rockfall event. To remove these anomalous objects, we first calculate the median and the median absolute deviation (MAD) of the rock positions for each time step. These statistical measures are chosen given they are less sensitive to outliers than the mean and standard deviation. We then convert the MAD to a standard deviation (σ) following

$$\sigma = 1.4826MAD \tag{1}$$

Rocks located more than 3σ from the median are discarded.

2.1.3 Initial conditions

A falling rock's initial position and velocity (speed and trend) has a notable effect on its subsequent trajectory (Crosta et al. 2015; Li and Lan 2015). Here, we use the mean position during the first time-step as the initial position. We then treat all measured rock positions of an event as a point cloud and use principal component analysis (Wold et al. 1987) to calculate the initial velocity. The first principal component, which captures the direction with the largest spatial variation of measured rock positions, is taken as the trend of the initial velocity. The initial speed is estimated as the standard deviation along this trend divided by the duration of the event. These initial positions and velocities are hereinafter termed seeders.

2.2 Rockfall simulations

We use a custom build of *RocFall3* from *Rocscience* that supports automated trajectory computation given an input file. Since the volume and shape of each falling rock is unavailable from radar-tracked data, we simulate the trajectories using a lumped-mass formulation and assume a volume of 1 m^3 for each seeder and a rock density of 2.7×10^3 kg/m^3. These parameters have a minimal impact on trajectory kinematics given that the rocks are idealized as point sources in a lumped-mass formulation. A digital terrain model (DTM) with a resolution of 0.65 meters is used to model the mine slopes.

2.3 Misfit

The relative completeness of the radar data allows us to measure the misfit between a measured and corresponding simulated rockfall trajectory for the entire trajectory, which offers better constraint than using individual features such as runout distance or bounce height. The misfit calculation comprises three steps: (1) computing the chi-square statistic to describe the misfit between trajectories, (2) converting into log-scale given that the misfits are approximately log-normal, and (3) min-pooling to emphasize the local minima in parameter space.

The chi-square statistic (Xie et al. 2024) can be defined as

$$\chi^2 = \sum_{i=1}^{N} \left[\frac{||\boldsymbol{u}_i - \hat{y}_i||}{\sigma_i}\right]^2, \tag{2}$$

where the variables $\boldsymbol{u}_i$, $\hat{y}_i$, σ_i are defined respectively as the mean measured rock position, simulated rock position, and standard deviation of the measured rock positions at time step *i*, as illustrated in Figure 3b. Here, the chi-square misfit is only computed for time steps preceding the cut-off time, which is defined as the end of the radar measurement. The runout time, when the velocity reaches zero, cannot be reliably obtained from the data because the monitoring is terminated if the rock exits the radar's field of view or decelerates below the detection threshold.

3 Results

Figure 4 illustrates the distribution of expected misfit obtained from the grid search, which represents the true distribution from an extensive brute-force search over 10,000 simulated trajectories. As illustrated by the green dots in the last row of Figure 4, the distribution of misfit resulting from grid search exhibits banding, which may be attributed to the chaotic nature of rockfall, where slight changes in the CORs result in distinctly different trajectories and misfit (Li and Lan 2015; Ignacio et al. 2021). Overall, the CORs of the entire site may be approximated as $R_n = 0.5 \pm 0.1$, $R_t = 0.65 \pm 0.2$, with the important caveat that there is notable negative covariance between R_n and R_t, indicating that similar trajectories can be simulated by increasing R_n and decreasing R_t, or vice versa.

Table 3 Mean (μ) and covariance (σ) of the CORs in the minimum highlighted green in Figure 4.

$\mu(R_n)$	$\mu(R_t)$	$\sigma(R_n)$	$\sigma(R_t)$	$\sigma(R_n, R_t)$
0.51	0.64	0.120	0.168	-0.01952

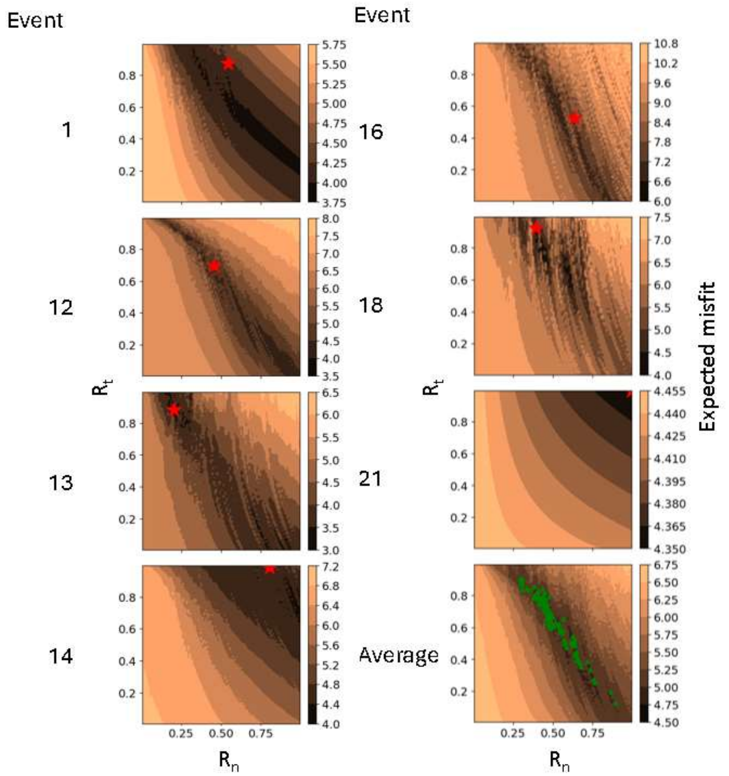

Figure 4 Coefficients of restitution for selected events and average of all events

To further examine the robustness of our model, we randomly draw 50 COR pairs from a bivariate normal distribution using the mean and covariance matrix from the site-wise analysis. The simulated trajectories corresponding to these COR pairs are illustrated in Figure 5. These simulated trajectories (yellow lines) all reasonably match the rockfall event data in terms of the overall trend (blue lines) and spread (marked by blue crosses).

4 Summary and conclusions

Well-constrained site-specific coefficients of restitution (CORs) are vital for reliable evaluation of rockfall hazards, with notable implications for the design of roadways, slopes, and mining benches. Recent developments in radar technology allow us to monitor these rockfall events at a spatial resolution on the order of meters and time resolution on the order of milliseconds. These data offer excellent opportunities for detailed back analysis of CORs governing the behavior of rockfall hazards. Here, we a grid search for back analysis of CORs and a case study of its application to a radar-measured rockfall catalog consisting of 21 events. Our key findings are:

1. We use a goodness-of-fit metric (Xie et al. 2024) to quantify the misfit between simulated and measured trajectories.
2. The 10000 simulations computed during the grid search shows distinct jumps in rockfall behaviour in the R_n-R_t parameter space, suggesting a chaotic system where small changes in rock-slope interactions can result in dramatic changes in rockfall trajectories.
3. We estimate average CORs of $R_n = 0.5 \pm 0.1$, $R_t = 0.65 \pm 0.2$. Rockfall trajectories simulated from this mean and covariance matrix show reasonable agreement with the measured trajectories.

Acknowledgements

We acknowledge funding from NSERC Alliance Grant ALLRP 576858-22 in partnership with Rocscience Inc. We would also like to thank Hexagon IDS Georadar for providing rockfall data.

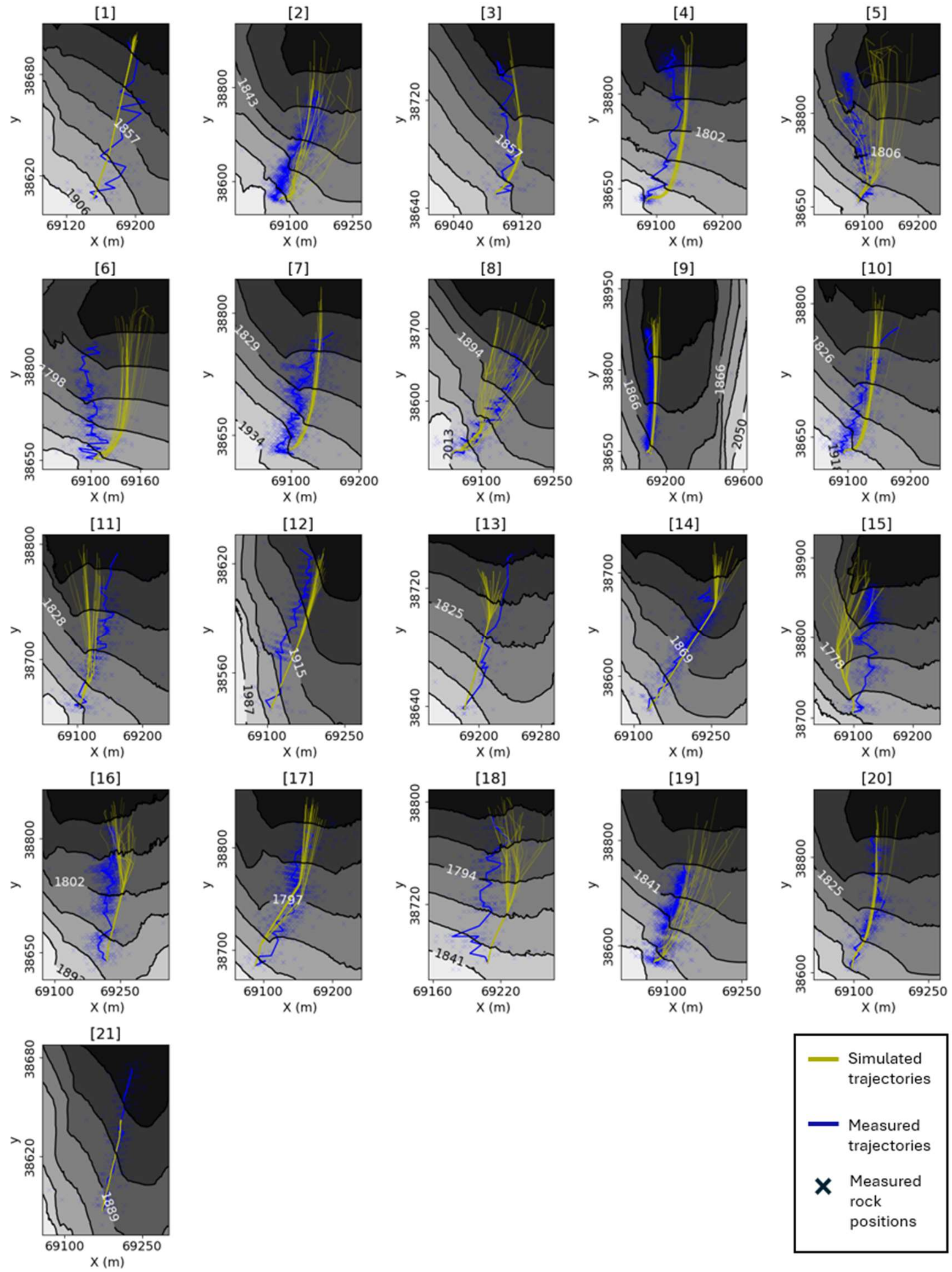

Figure 5 Fifty best-fitting simulated trajectories for each event

References

Blahůt J, Racek O (2023) Modern Methods of Rock Mass Characterisation and Rockfall Monitoring: A Review. In: Thambidurai P, Singh TN (eds) Landslides: Detection, Prediction and Monitoring: Technological Developments. Springer International Publishing, Cham, pp 1–38

Bonneau DA, Hutchinson DJ, DiFrancesco P-M, et al (2019) Three-dimensional rockfall shape back analysis: methods and implications. Natural Hazards and Earth System Sciences 19:2745–2765. https://doi.org/10.5194/nhess-19-2745-2019

Budetta P, De Luca C, Nappi M (2016) Quantitative rockfall risk assessment for an important road by means of the rockfall risk management (RO.MA.) method. Bull Eng Geol Environ 75:1377–1397. https://doi.org/10.1007/s10064-015-0798-6

Carlà T, Gigli G, Lombardi L, et al (2024) Real-time detection and management of rockfall hazards by ground-based Doppler radar. Landslides 21:155–163. https://doi.org/10.1007/s10346-023-02144-1

Carlà T, Nolesini T, Solari L, et al (2019) Rockfall forecasting and risk management along a major transportation corridor in the Alps through ground-based radar interferometry. Landslides 16:1425–1435. https://doi.org/10.1007/s10346-019-01190-y

Castelli M, Torsello G, Vallero G (2021) Preliminary Modeling of Rockfall Runout: Definition of the Input Parameters for the QGIS Plugin QPROTO. Geosciences 11:88. https://doi.org/10.3390/geosciences11020088

Caviezel A, Ringenbach A, Demmel SE, et al (2021) The relevance of rock shape over mass—implications for rockfall hazard assessments. Nat Commun 12:5546. https://doi.org/10.1038/s41467-021-25794-y

Crosta GB, Agliardi F, Frattini P, Lari S (2015) Key Issues in Rock Fall Modeling, Hazard and Risk Assessment for Rockfall Protection. In: Lollino G, Giordan D, Crosta GB, et al. (eds) Engineering Geology for Society and Territory - Volume 2. Springer International Publishing, Cham, pp 43–58

Fanos AM, Pradhan B (2018) Laser Scanning Systems and Techniques in Rockfall Source Identification and Risk Assessment: A Critical Review. Earth Syst Environ 2:163–182. https://doi.org/10.1007/s41748-018-0046-x

Fanos AM, Pradhan B (2016) Multi-scenario Rockfall Hazard Assessment Using LiDAR Data and GIS. Geotech Geol Eng 34:1375–1393. https://doi.org/10.1007/s10706-016-0049-z

Ferrari F, Giacomini A, Thoeni K (2016) Qualitative Rockfall Hazard Assessment: A Comprehensive Review of Current Practices. Rock Mech Rock Eng 49:2865–2922. https://doi.org/10.1007/s00603-016-0918-z

Ignacio FV, De Menezes Filho AP, Castro Fontenla Sieira AC (2021) Analogy to the chaos theory applied to the study of rockfalls. S&R 44:1–9. https://doi.org/10.28927/SR.2021.059420

Jaboyedoff M, Ben Hammouda M, Derron M-H, et al (2021) The Rockfall Failure Hazard Assessment: Summary and New Advances. In: Sassa K, Mikoš M, Sassa S, et al. (eds) Understanding and Reducing Landslide Disaster Risk: Volume 1 Sendai Landslide Partnerships and Kyoto Landslide Commitment. Springer International Publishing, Cham, pp 55–83

Jele R, Sullivan T (2016) Slope design at Mt Rawdon gold mine. In: Proceedings of the First Asia Pacific Slope Stability in Mining Conference. Australian Centre for Geomechanics, Perth, pp 353–364

Li L, Lan H (2015) Probabilistic modeling of rockfall trajectories: a review. Bull Eng Geol Environ 74:1163–1176. https://doi.org/10.1007/s10064-015-0718-9

Mineo S (2020) Comparing rockfall hazard and risk assessment procedures along roads for different planning purposes. J Mt Sci 17:653–669. https://doi.org/10.1007/s11629-019-5766-3

Mirhadi N, Macciotta R (2023) Quantitative correlation between rock fall and weather seasonality to predict changes in rock fall hazard with climate change. Landslides 20:2227–2241. https://doi.org/10.1007/s10346-023-02105-8

Noël F, Nordang SF, Jaboyedoff M, et al (2023) Comparing Flow-R, Rockyfor3D and RAMMS to Rockfalls from the Mel de la Niva Mountain: A Benchmarking Exercise. Geosciences 13:200. https://doi.org/10.3390/geosciences13070200

Peik B, Zare Naghadehi M, Battulwar R, et al (2020) An Analytical Study of Rockfall Trajectory Simulation to Develop Hazard Maps for Open-Pit Mines. OnePetro

Pieraccini M, Noferini L, Mecatti D, et al (2006) Integration of Radar Interferometry and Laser Scanning for Remote Monitoring of an Urban Site Built on a Sliding Slope. IEEE Transactions on Geoscience and Remote Sensing 44:2335–2342. https://doi.org/10.1109/TGRS.2006.873574

Pierson LA, Davis SA, Van Vickle R (1990) Rockfall Hazard rating system: implementation manual

Potter J, Meyer B, Ross B, et al (2024) Development of a Prototype Thermal Imaging Rockfall Detection System. OnePetro

Sabatakakis N, Depountis N, Vagenas N (2015) Evaluation of Rockfall Restitution Coefficients. In: Lollino G, Giordan D, Crosta GB, et al. (eds) Engineering Geology for Society and Territory - Volume 2. Springer International Publishing, Cham, pp 2023–2026

Scavia C, Barbero M, Castelli M, et al (2020) Evaluating Rockfall Risk: Some Critical Aspects. Geosciences 10:98. https://doi.org/10.3390/geosciences10030098

Silveira LRC, Lana MS, dos Santos TB (2024) A Quantitative Rockfall Risk Analysis System for Highway Rock Slopes. Geotech Geol Eng 42:1131–1152. https://doi.org/10.1007/s10706-023-02609-z

Soler L, Wieber F, Allamel-Raffin C, et al (2013) Calibration: A Conceptual Framework Applied to Scientific Practices Which Investigate Natural Phenomena by Means of Standardized Instruments. J Gen Philos Sci 44:263–317. https://doi.org/10.1007/s10838-013-9231-7

Stoffel M, Trappmann DG, Coullie MI, et al (2024) Rockfall from an increasingly unstable mountain slope driven by climate warming. Nat Geosci 17:249–254. https://doi.org/10.1038/s41561-024-01390-9

Teza G, Marcato G, Pasuto A, Galgaro A (2015) Integration of laser scanning and thermal imaging in monitoring optimization and assessment of rockfall hazard: a case history in the Carnic Alps (Northeastern Italy). Nat Hazards 76:1535–1549. https://doi.org/10.1007/s11069-014-1545-1

Viani C, Chiarle M, Paranunzio R, et al (2020) An integrated approach to investigate climate-driven rockfall occurrence in high alpine slopes: the Bessanese glacial basin, Western Italian Alps. J Mt Sci 17:2591–2610. https://doi.org/10.1007/s11629-020-6216-y

Viviani F, Michelini A, Mayer L (2020) RockSpot: an Interferometric Doppler Radar for Rockfall/Avalanche Detection and Tracking. In: 2020 IEEE Radar Conference (RadarConf20). pp 1–5

Williams C, Morkeh J, Dorfschmidt K, et al (2020) Innovative Rockfall Solutions Based on Calibration and Field Testing. Mining, Metallurgy & Exploration 37:101–116. https://doi.org/10.1007/s42461-019-0092-4

Wold S, Esbensen K, Geladi P (1987) Principal component analysis. Chemometrics and Intelligent Laboratory Systems 2:37–52. https://doi.org/10.1016/0169-7439(87)80084-9

Wu S-S (1984) Rockfall evaluation by computer simulation. Transportation research record 1031:1–5

Wyllie DC (2014a) Calibration of rock fall modeling parameters. International Journal of Rock Mechanics and Mining Sciences 67:170–180. https://doi.org/10.1016/j.ijrmms.2013.10.002

Wyllie DC (2014b) Rock Fall Engineering. CRC Press, Boca Raton

Xie AY, Huang Z, Yacoub T, Li BQ (2024) Quantification of uncertainties in back-analysis of radar-tracked rockfall trajectories. Journal of Rock Mechanics and Geotechnical Engineering. https://doi.org/10.1016/j.jrmge.2024.08.001

Zhao L, Jin C, Huang D, et al (2024) Rockfall analysis considering coefficients of restitution based on three-dimensional sphere discontinuous deformation analysis. Bull Eng Geol Environ 83:460. https://doi.org/10.1007/s10064-024-03973-7

Zheng L, Zhu Z, Wei Q, et al (2021) A Stochastic Rockfall Model Related to Random Ground Roughness Based on Three-Dimensional Discontinuous Deformation Analysis. Front Earth Sci 9:. https://doi.org/10.3389/feart.2021.819751

Zhu Z, Zeng B, Zhao H, et al (2024) Structure plane interpretation of rockfall and early identification of potential hazards based on UAV photogrammetry. Nat Hazards. https://doi.org/10.1007/s11069-024-06881-x

(1943) Radio Detection and Ranging. Nature 152:391–392. https://doi.org/10.1038/152391b0